Journal of materials and Environmental Sciences
ISSN : 2028-2508

JMES, 2017 Volume 8, Issue 1, Page 264-272
http://www.jmaterenvironsci.com/

Features of the low–level temperature inversions at Abidjan upper-air station (Ivory Coast)

F. K. Guédjé*, V. V. A. Houéto, E. Houngninnou
Laboratoire de Physique de l'Atmosphère, Faculté des Sciences et Techniques, Université d'Abomey-Calavi, 01 BP 4521 Cotonou, Bénin.

Received 16 May 2016,
Revised 04 Nov 2016,
Accepted 06 Nov 2016

Keywords

- radiosonde,
- meteorology,
- inversion,
- air pollution,
- Abidjan upper-air

F. K. Guédjé
guedjefranco@yahoo.com
Phone: +22994958988

Abstract

This work examine the characteristics of the low-level (surface-based and elevated) temperature inversions above Abidjan (Ivory Coast) to a pressure level of 700 hPa by using daily (midnight and midday) upper-air meteorological data over the period 2007-2015. The monthly and vertical variations of inversions, characterized by vertical gradients of temperature (strength), potential temperature, dew point temperature, depth, and inversion index, were studied. On the monthly basis, it is worth noting that elevated inversions were more common throughout the year than surface-based inversions. The frequency peak of elevated inversions was found in summer months whereas the peak of surface-based was in winter. Moreover, for the both midday and midnight soundings, the strongest inversions occurred in summer but a relative maximum strength of inversions was evidently shown in winter. The vertical variations of the characteristics of inversions helped us to highlight the types of inversions and the physical processes associated. The role of radiation inversions for air pollution dispersion was also discussed.

1. Introduction

Concentration of key air pollutants depends strongly upon the stability conditions in the lower atmosphere. Thermal inversions, atmospheric stability, and mixed layer height are probably the most important meteorological conditions controlling atmospheric pollution dispersion [1]. Many studies on the effect of atmospheric conditions on air pollution related air pollution episodes with temperature inversions [2, 3, 4, 5] and several of the inversion climatologies are restricted to the surface inversions or the first elevated inversions [6, 7, 8] as above the 700 hPa pressure level, both the frequency of occurrence and the mean potential temperature difference of inversions decrease very rapidly [9] and above 400 hPa, many inversions were found to be associated with the tropopause [10]. The first stable layer encountered in a temperature profile is, in many cases, an inversion layer and is important at the local scale, as it plays a central role in controlling air pollution dispersion [10]. Indeed, the nocturnal cooling of the ground is the main factor for the occurrence of the radiational inversion, with its base-height at the surface of the Earth (i.e. surface-based inversion). However, depending upon the large-scale synoptic meteorological forcing, an upper level thermal inversion can also exist topping the local Atmospheric Boundary Layer (ABL).
The ABL is the lowest part of the troposphere in permanent contact with the Earth's surface and responds to thermal and roughness surface forcing in timescales of minutes to hours [11]. Its state is conditioned by synoptic large-scale meteorological processes like horizontal air mass exchange for example under a cyclonic air mass advection [12] or an adiabatic compression through the formation of a high pressure anticyclone, on upper tropospheric levels [13, 14]. These large-scale synoptic processes constrain the temperature of the air mass in tropospheric levels without initial connection to the local surface temperature forming vertically localized positive upward thermal gradients called elevated inversion layers [15, 16]. Hence, subsidence inversions occur due to higher level, broad-scale sinking motions associated with high pressure systems along with lower level turbulence within the surface mixed layer [17]. The subsidence inversion will then be below the level of zero horizontal divergence where the vertical velocity will be maximized [10]. At daytime, elevated inversions are caused not only by subsidence but also by turbulence (turbulence inversion) that cools the air just below them owing to adiabatic expansion [10].

The climatology of the both surface-based and elevated inversions are found in the literature and are described by several authors using data from radiosondes [6, 7, 8]. Very few descriptions of temperature inversions have been made in West African coastal regions. Given the typical feature of the atmosphere of these regions, characterized by high activities of subtropical anticyclones of Azores in winter and St Helena in summer, high surface temperatures in summer inducing turbulent mixing in the ABL and an increased nocturnal cooling of Earth's surface during winter clear nights, the study of low level temperature inversions should highlight important features to be described. However, the lack of upper-air soundings over relatively long periods at the West-African coastal stations is an important issue. Because of the importance of the inversion layers and their link with pollutions, it is worth noting to study their behavior and the variations in their general characteristics. The present work is one of the first known investigation that address the analysis of the thermal inversions in Abidjan. In this paper a comprehensive study on the diurnal cycle of inversion layers characteristics up to 700 hPa including their frequency of occurrence, depth, strength, intensity and their physical origin, using radiosonde data from Abidjan upper-air station will be undertaken, aiming to examine the effect of local factors and large scale synoptic conditions.

2. Data and methodology

This study is based on the statistical analysis of the upper air data collected over a period of nine years from 2007 to 2015. Abidjan, as shown in figure 1, is situated in the west–african coastal region (5°15' N, 3°55'W) at an elevation of 8 m, in an extensive area of low relative relief.

The radiosonde data are extracted from the NOAA's Integrated Global Radiosonde Archive (IGRA) which consists of radiosonde and pilot balloon observations at over globally distributed stations. In order to study the diurnal cycle of low-level temperature inversions, both daytime and nighttime radiosonde are needed. Except Abidjan upper-air station located at the international airport, there is no other station at the Guinean coast that continuously provides available daily radiosonde data (midday and midnight); soundings in Lagos, Cotonou, Lome or Accra either stopped several years ago or were non-homogeneous. Although in Abidjan there is a lack of data between 2000 and 2007, except this period, the radiosonde data are quasi-continuous as shown in figure 2 which represents the monthly series of the total number of soundings from 2000 to 2015. It can be noted that more than 60% (respectively 80%) of the midday and midnight soundings have an average monthly number of observations greater than 25 over 30 (respectively 15 over 30). This looks like a good score, given the difficulties related to the upper-air soundings in the region.

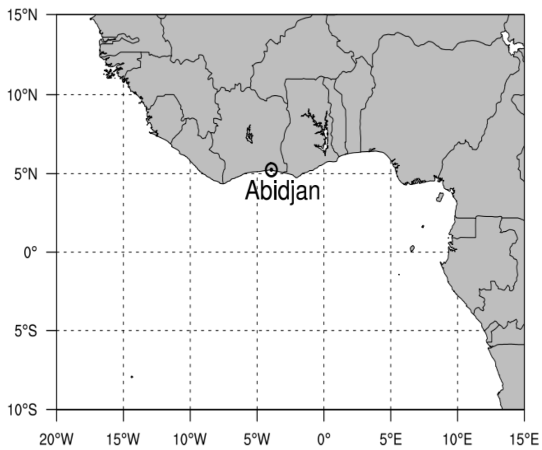

Figure1: Geographical location of Abidjan.

The data are based on the so-called significant levels, between surface and 700 hPa for the both midday and midnight soundings. Variables include pressure, temperature, geopotential height, dew point depression, wind direction and wind speed (for further details on the data, see the NOOA's website). The isobar level of 700 hPa is chosen as the reasonable upper limit for the study of the tropospheric inversion climatology as above that pressure level both the frequency of occurrence and the mean potential temperature difference of inversions decrease very rapidly [9]; where adjacent inversions were found, they were merged together to give a deeper inversion.

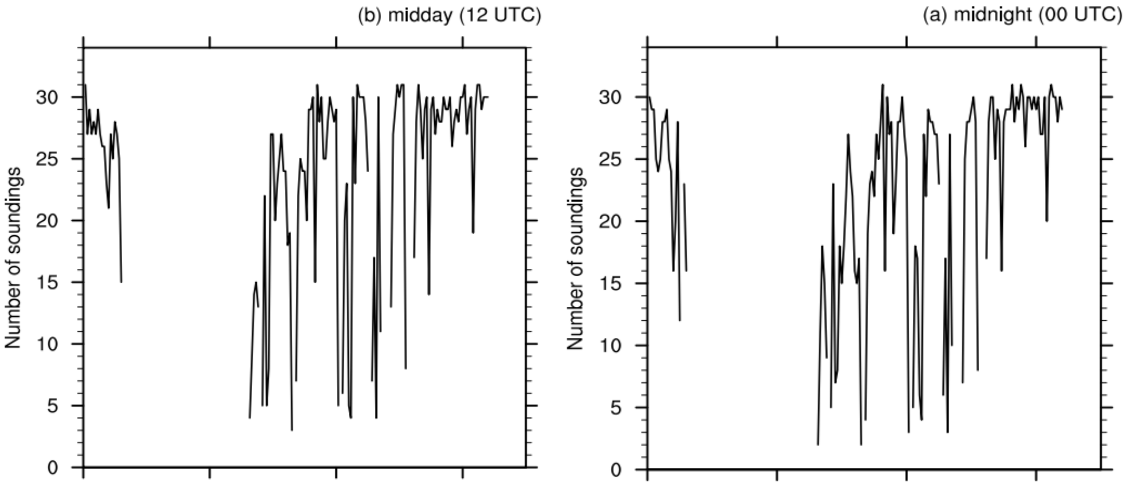

Figure2: Monthly time series of the number of (a) midnight and (b) midday soundings at Abidjan upper-air station.

For each layer that contains an inversion, the height of inversion base *Hb*, the depth of the inversion layer (ΔH: difference in altitude between the top and the base of the inversion), and the strength of the inversion (ΔT : difference in the dry-bulb temperatures between the top and the base of the inversion) are computed. In addition, two more properties are taken into account: the difference in dew point temperature between the top and the base of the layer (ΔTd) and the difference in potential temperature between the top and the base ($\Delta\theta$), called “intensity” of inversion. The intensity of inversions is directly proportional to their ability to inhibit the vertical movement of pollutants [10]. So, $\Delta\theta$ is an important variable, particularly from the point of view of air pollution, since it denotes the ability of the inversion to inhibit vertical diffusion throughout its depth [10]. The value of ΔTd is a potential indicator of the physical origin of an inversion. Within anticyclonic subsidence inversions the dew point temperature decreases with height [18], and in frontal inversions, depending on the type of frontal inversion, it usually increases [19].

In this study, emphasis is placed on the monthly variation of the characteristics of temperature inversions to bring out their seasonal fluctuations. As the period covered by the study is not too long, interannual variations are not taken into account although they could give important indications about the impact of climate variability on inversions. So, the temperature profile data are derived and tabulated on a monthly basis. The statistical analysis of the temperature data is performed to determine the type, height, strength and intensity of the thermal inversions in the period covered by the study. Temperature inversions are identified using the detection algorithm developed by [20]. To find the frequencies with which surface-based and elevated inversions occur each month, the equations described by [21] are used:

$$N_{inv} = N_{elev} + N_{SBI} \tag{1}$$

$$F_{elev} = \frac{N_{elev}}{N_{inv}} \tag{2}$$

$$F_{SBI} = \frac{N_{SBI}}{N_{inv}} \tag{3}$$

$$F_{all} = \frac{N_{inv}}{N_{all}} \tag{4}$$

where F_{elev}, F_{SBI} and F_{all} are respectively the frequency of occurrence of elevated, surface-based and all inversions, N_{elev} and N_{SBI} are respectively the number of elevated and surface-based inversions, N_{inv} is the total number of inversions, and N_{all} is the total number of soundings including those soundings in which an inversion was not detected. Therefore, although F_{all} is the frequency of occurrence of all inversions, F_{elev} and F_{SBI} are the frequency with which inversions, when present, are elevated or surface-based respectively [21]. For each sounding profile, it was possible to find several layers of temperature inversions. Hence, when considering a certain period of time (e.g. monthly), N_{inv} could be greater than N_{all}, so that F_{all} could possibly be greater than 100%.

Then, a method utilized by Milionis and Davies (1992) is experienced: the atmosphere is separated into layers of 50 hPa each, from surface up to the 700 hPa pressure level, to study the vertical variation and the diurnal cycle of the inversions characteristics. For each layer the mean ΔT , ΔH, ΔT_d, and $\Delta\theta$ are calculated and plotted as a function of the mean pressure of the layers. A simple index, defined by the authors, given by the product of the mean $\Delta\theta$ at the layer and the number of inversions in the layer, is used to combine the frequency and the intensity of the inversions.

3. Results and discussion

Figures below depict the monthly variation and the vertical variation of the main characteristics of temperature inversions at Abidjan upper–air station. The standard deviations calculated for each parameter are not drawn in any of the figures that will be presented later in order to avoid unnecessary complexity.

3.1. *Monthly variations of the temperature inversions characteristics*

Figure 3 shows the monthly averaged frequency of surface-based inversions, elevated inversions and all inversions, calculated using the expressions from (1) to (4) above.

Throughout the year, the surface-based inversions are more common than the elevated inversions. In general, the midday variation in the frequency of surface-based and elevated inversions does not show any evident particularity. At midnight, it can be seen that surface-based inversions are more common in winter months and there is a decreasing trend from January to October. The nocturnal maximum frequency of the surface-based inversions during winter months is closely related to the diurnal amplitude of surface temperature. This can be explained by clear skies during winter nights that promote cooling at the surface and by the relative stability in the boundary layer that reduce turbulent mixing. Such conditions could allow surface-based inversions to persist undisturbed for longer periods during the winter. In turn, in summer months, cloudy skies during nights and turbulent mixing in the ABL at daytime result in a reduced frequency of surface-based inversions and produce turbulent inversion in altitude that increase the frequency of elevated inversions. The two inversion types have opposite frequency trends, each type favored by different atmospheric conditions.

Moreover, a clear change in the frequency of all inversions is evident in winter (December–January) and in summer (July–August–September) when the maxima are reached. This is due to the frequency peak of surface-based inversions and elevated inversions in winter and summer months respectively. The monthly variation of the mean strength and the mean depth of all inversions are shown in figures 4 (a) and (b). The strongest inversions occur in summer (1.35°C at midday, 1.15°C at midnight), with another relative maximum strength in winter (0.95°C at midnight, 0.82°C at midday) and match well with the maximum frequencies described earlier. In summer where elevated inversions are more common, the midday strength is greater than the midnight strength. Indeed, the frequency of elevated inversions (of anticyclonic origin) is increased by turbulence and convective inversions generated by the turbulent mixing observed in daytime. On the other hand, in winter, inversions are stronger at midnight only in January and this is due to the effect of surface-based inversions which frequency increases in January in comparison with their summer frequency values. Hence, the frequency increasing of midnight surface-based inversions in winter (figure 3 (a)) was not enough to maintain the midnight inversions stronger than the midday inversions throughout the winter. In figure 4 (a), the behavior of both profiles observed between December and May is different from that observed between May and November where inversions are stronger at midday than at midnight. While in January the increasing in the frequency of surface-based inversions raised the strength of midnight inversions, this is not the case in February and March where inversions were rather stronger at midday than at midnight. On the other hand, in April, theses inversions become stronger again at daytime than at nighttime. Indeed, figure 3 (a) shows that the frequency of all inversions is low in April. Even if inversions are more frequent at daytime than at nighttime (figure 3 (a)), they are not stronger at midday than at midnight (figure 4 (a)) where the average difference of temperature reaches 0.75°C. In spite of the erratic behavior of both profiles between December and May in figure 4, it is clear that the strength and the frequency of all inversions highlight a marked diurnal cycle in relation to the turbulent mixing at daytime and the radiational cooling at night in lower levels of the atmosphere. The types of inversions and their physical origin are more discussed in the next subsection.

Similarly, at midday, the deepest inversions occur in winter (133 m) and in summer (160 m) whereas the minimum depth occurred in March (110 m). The same profile was observed earlier for the strength and this could suggest that the greater the temperature difference ΔT, the larger the depth ΔH, as it is shown in Figure 4 where there seems to be a linear regression between ΔT and ΔH with a significant (5% level) correlation coefficient equal to 65,05%.

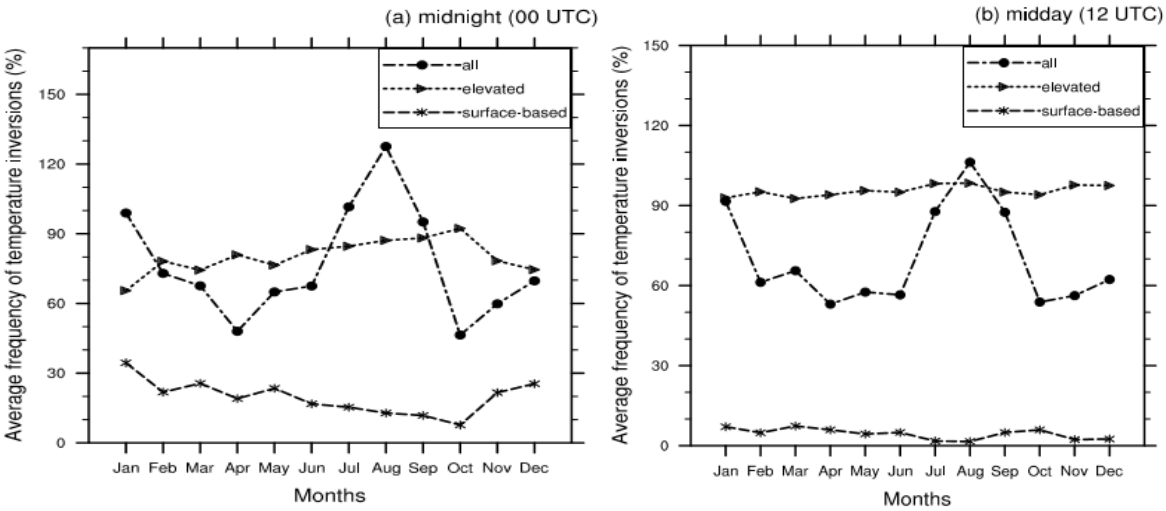

Figure3: Monthly averaged frequency (2007 – 2015) of surface-based, elevated, and all inversions (%) at Abidjan.

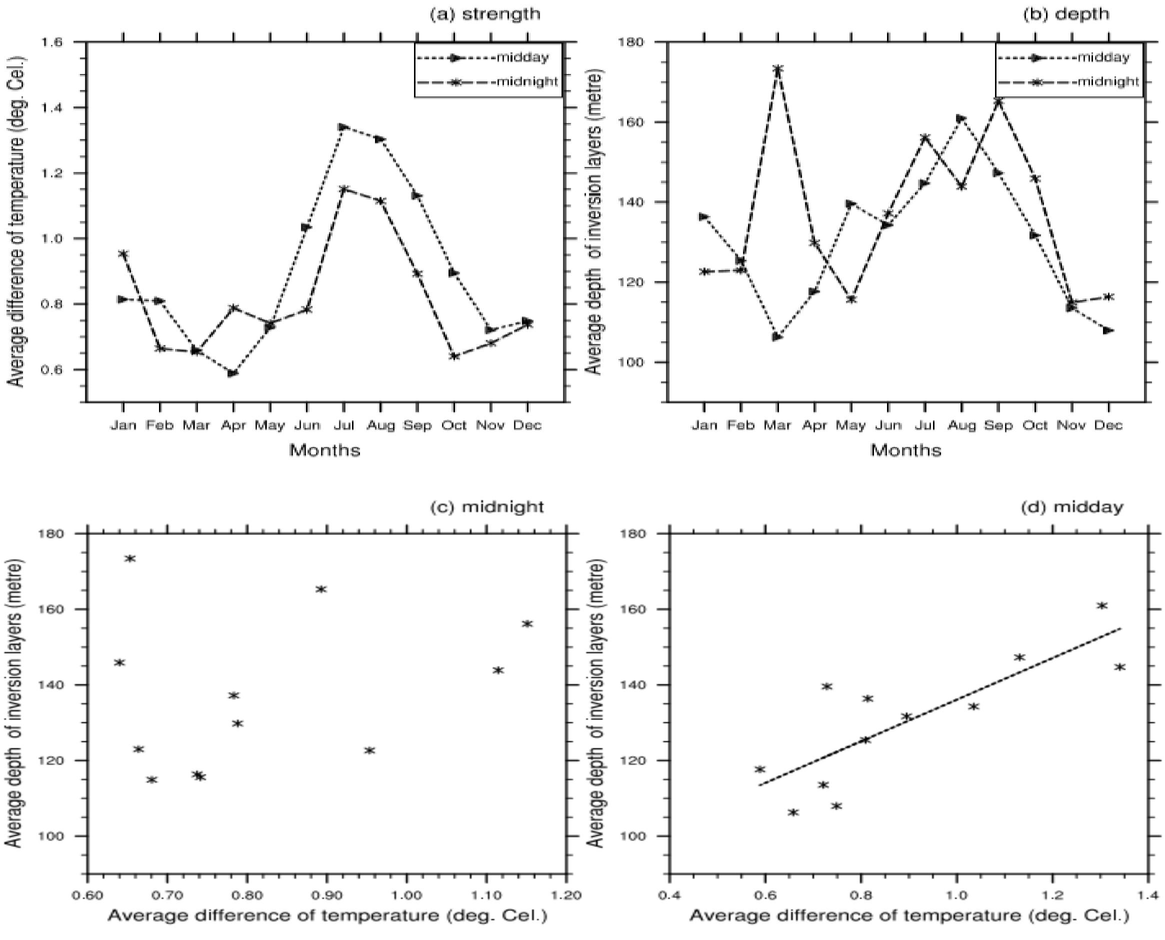

Figure4: Monthly averaged (a) strength and (b) depth over 2007 – 2015 of all inversions at Abidjan; variation of strength as a function of depth at (c) midnight and (d) midday over 2000–2015 at Abidjan.

The differences between the midnight and midday depth profiles are the deepest inversion observed in March (173 m), the slightly decrease in ΔH observed in August, and the relatively high depth in October (145 m) which make the both profiles not correlated (figure 4(c)). The origin of the high value of ΔH noted in March could come from atmospheric conditions observed in that period especially during night; this could be an interesting feature to be studied, but it was not discussed here.

3.2. *Vertical variations of the temperature inversions characteristics*

Figure 5 shows the vertical variation of the intensity $\Delta\theta$ for each layer. $\Delta\theta$ has maximum values in the layers 850-800 hPa and 800-750 hPa. The same layers accommodate the maximum values of the number of inversions (figure 6), and consequently the maximum values of the inversion index (figure 7). However, examination of the vertical variation of ΔTd (figure 8), shows that there is a pronounced minimum at the layers 850-800 hPa and 800-700 hPa. This implies that inversions in these layers are subsidence inversions mostly of anticyclonic origin and, to a lesser extent, of turbulent mixing.

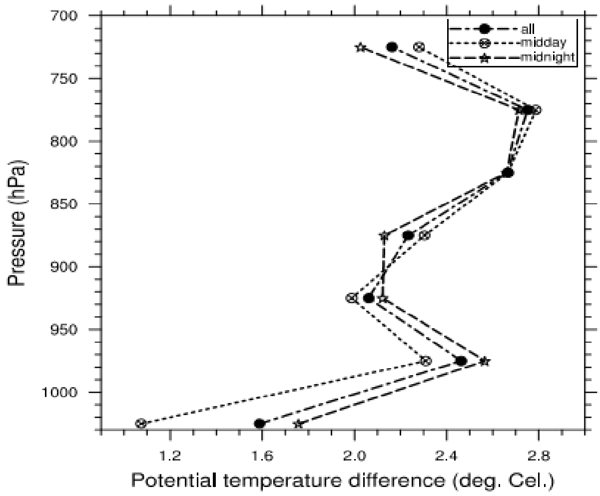

Figure5: Vertical variation of the mean potential temperature difference Δθ in inversion layers.

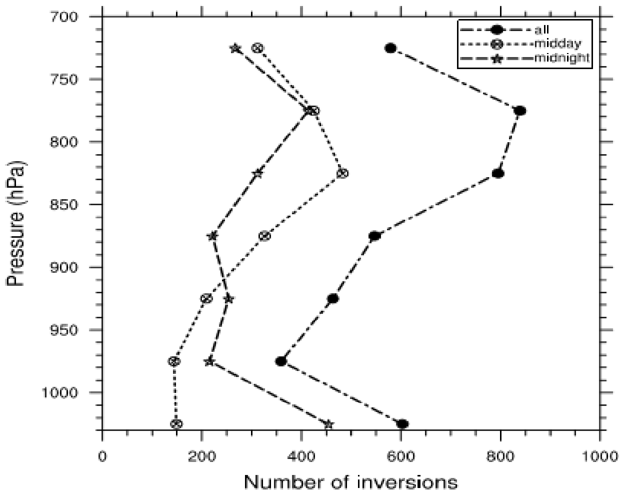

Figure6: Vertical variation in the mean number of inversions in each 50 hPa-depth inversion layer.

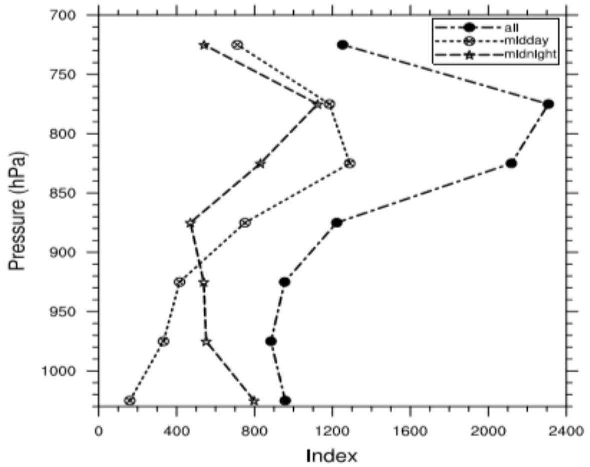

Figure7: Vertical variation of the inversion index.

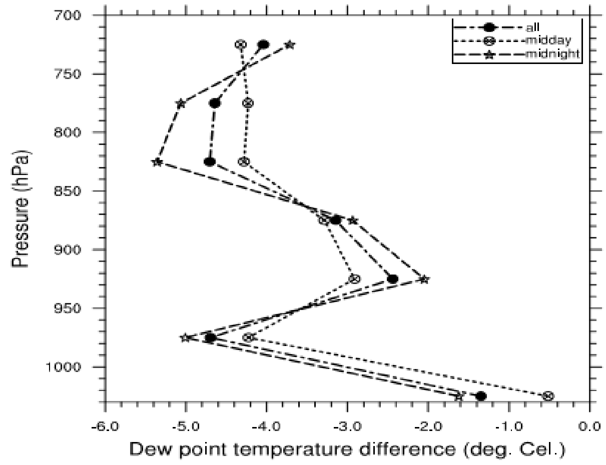

Figure8: Vertical variation of the mean dew point temperature difference ΔTd in inversion layers.

Nevertheless, it is interesting to notice that the number of inversions in the layers 900-850 hPa and 850-800 hPa at midday is higher than at midnight. This difference in the number of inversions for midday and midnight can be explained by the absence of turbulence inversions at midnight. So, the elevated inversions at midday are caused not only by anticyclonic subsidence, but also by turbulence mixing in the ABL. Typical heights of daytime convective ABLs are about 1000-1500 m [22, 11], which roughly corresponds to 900-850 hPa. It is at these heights that the base of turbulence inversions is often located. In the process of vertical mixing the air carried upward is cooled adiabatically.

Similarly the air brought downwards heated at the same adiabatic rate. After a prolonged mixing in the atmosphere, the air at the maximum height of turbulent penetration becomes colder than what it was before, and that at the bottom of the turbulence layer will be warmer than what it was originally. The transition from this cold upper part of the turbulence zone to the air above with its temperature unaffected by adiabatic cooling comprises a temperature inversion. It is worth noting that in the layers 1000-950 hPa and 950-900 hPa the number of inversions is much higher at midnight than at midday in contrary to earlier descriptions in the layers 900-850 hPa and 850-800 hPa just above. At midnight, as the ABL is stable on average, turbulence at midnight is much weaker than at midday and in the absence of anticyclonic subsidence, the turbulence inversion that is present during the day may disappear at midnight [10]. When anticyclonic subsidence conditions are present, the subsidence capping inversions of midday are not expected to be destroyed during the night, but instead to extend further towards the ground and perhaps strengthen as turbulence weakens [10]. So, these subsidence inversions, as they move lower during the night, are found and counted in the layers 1000-950 hPa and 950-900 hPa, sometimes are merged with the ground radiation inversions and, hence, increase the frequency of occurrences at these layers. The ΔTd profile, which is not a monotonic function of height but has a point of inflection in low levels (around 950 hPa) reflects this phenomenon: below the height where the point of inflection is located, the inversion is due to radiation and, above the point of inflection, it is due to subsidence [10].

At the ground surface, the intensity $\Delta\theta$ is lowest whereas the number of inversions exhibits a relative maximum. The index which is the combination of these two properties, slightly increases only at night. This last result shows that in the layers Ground-1000 hPa and 1000-950 hPa, the temperature inversions noted are mostly radiational.

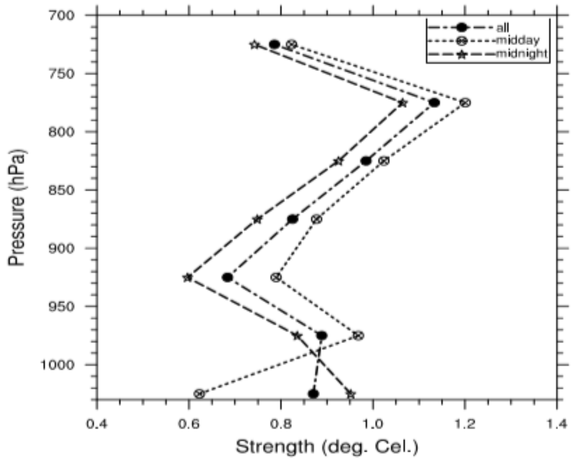

Figure9: Vertical variation of the mean strength ΔT of inversion layers.

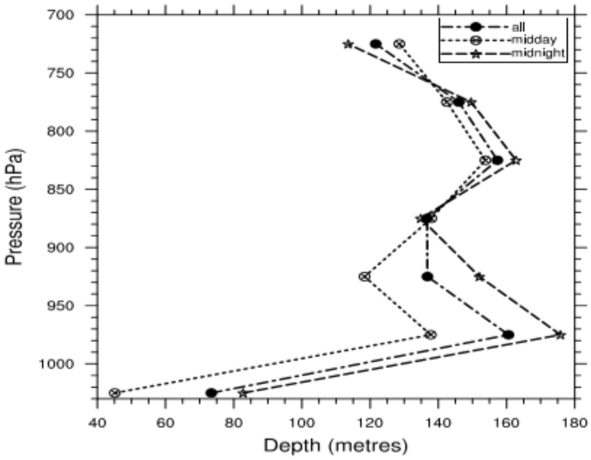

Figure10: Vertical variation of the mean depth ΔH of inversion layers.

The surface-based inversions (Ground-1000 hPa) are more frequent but less intense whereas the inversions in the layer 1000-950 hPa are much less frequent but more intense. The inversions in the layer 1000-950 hPa could, therefore, be described at midnight as the combination of surface-based inversions and downwards turbulence inversions on the one hand, and at midday as the persistence of surface-based inversions, on the other hand.

Figure 9 depicts the vertical variation of inversion strength ΔT. At midday and midnight the strongest inversions are found in the layer 800-750 hPa (1 - 1.2°C). The inversion strength is lower at midnight than at midday, except at surface due to radiational inversions at night. Hence, it is evident that the weakest inversions at midday be located at surface (0.6°C), so that the layer 1000-950 hPa shows a relative maximum (1 °C). At midnight the minimum strength of inversions is found in the layer 950-900 hPa (0.6°C) which looks like a “ transition layer” between subsidence and radiational inversions.

In all cases, figure 10 shows that the both subsidence and turbulence inversions are deep (up to 160 m) and surface-based inversions are shallow (on average, 80 m maximum) at midday and midnight. However, in the layer 1000-950 hPa there is an increasing trend of depth despite the low number of inversions. In this layer where the deepest inversion at midnight (175 m) and a relative maximum depth at midday (140 m) are located, the types of inversions was described earlier and the fluctuations of $\Delta\theta$ and ΔTd tend to confirm these depth high values. Simultaneous determination and characterization of elevated and surface-based inversions has the potential to improve assessment on local air pollution meteorology [23]. Surface-based inversions play a major role in air pollution, especially during the winter when these inversions are strong in Abidjan. As pollutants from vehicles, fireplaces and industry are emitted into the air, the inversion traps these pollutants near the ground, leading to air poor quality. Moreover, during the winter months the seasonally variable Harmattan current transports large amounts of mineral dust at irregular intervals from the Chad Basin to the Sahel and Guinean coast where it reduces visibility, relative humidity and temperatures [24, 25]. This is one of the most important source of air pollution in winter at West-African coastal regions and the persistence of surface-based inversions increases the phenomenon. The aerosol concentrations cause irritation of respiratory tracts, and visibility reduction in car and air traffic that represent a serious problem during dust events.

For instance, air pollution meteorology and pollutant transport processes are strongly dependent on meteorological conditions [26], in both the vertical (low value of inversion index) and the horizontal (strong winds) directions [10]. Strong winds near ground surface are often related to low-level nocturnal jets. [27] showed that nearly all year round, nocturnal low level jets occur with more or less intensity over several locations in West Africa and can peak up to 15–20 m/s below 500 m above ground level. The speed and depth of the low level jet depend on a range of factors, including baroclinity, terrain slope, surface cooling rates and many more [28, 29]. So, the height of the nocturnal jet is located in the layer 1000-950 hPa, where the frequency of inversions is much greater at midnight than at midday. A region of strong wind shear (related to the nocturnal jet) and stable stratification (due to the radiation inversion) should occur just above the nocturnal surface-based inversion (80 m on average) and below the (nocturnal) low level jet (500-600 m on average), where conditions for the diffusion of pollutants are favourable.

Conclusion

Abidjan meteorological station located at the international airport, experienced both surface-based and elevated inversions although elevated inversions were more common throughout the year. For all characteristics (frequency, depth, strength), the monthly variation showed a marked diurnal cycle mainly related to the physical processes associated with the inversions formation.

Depending upon the types of inversions and the physical processes associated, the atmosphere above the site included three main zones in constant interaction:

• The first begin from 800 to 700 hPa where subsidence inversions within anticyclones were predominant. Their frequency, strength, depth and intensity showed in general extreme values.

• The second zone from 900 to 800 hPa showed a monotonic variation in the inversions characteristics, and a pronounced diurnal cycle influenced by turbulent mixing in the ABL which effects produced turbulence inversions at daytime that could affect lower layers (1000-900 hPa) during night.

• The third zone between surface and 950 hpa where surface-based inversions were found, induced by radiational cooling of ground surface at night, depicted evidently different characteristics from daytime to night.

Except subsidence inversions in the layers 800–700 hPa, the diurnal cycle is much pronounced from ground surface to 800 hPa, where the nocturnal terrestrial radiation and the daytime turbulent mixing in the ABL strongly influenced the frequency, strength, depth and intensity of all types of inversion. The most conspicuous effect is located at surface where the midnight characteristics of surface-based inversions in winter could play an important role for the air pollution dispersion. Overall, this work provided useful information about the characteristics of the thermal inversions in Abidjan and examined the impact of the local inversion layers on the air pollution dispersion, in a country witnessing a rapid rate of urban and industrial growth. Like in Abidjan, West-African coastal cities are experiencing a rapid urban growth and a comprehensive study of the phenomenon should help to assess the spatial character of inversion climatology in the region and better plan industrial activities.

Acknowledgment-The authors would like to thank A. Fink and P. Knippertz from Karlsruhe Institute of Technology (KIT) through the DACCIWA project.

References

1. Tunner D. B., *U.S. Environ. Prot. Agency*, Research Triangle Park, N. C. (1970).
2. Janhall S., Olofson K.F.G., Andersson P. U., Pettersson J. B. C. and Hallquist M, *Atmos Environ.*, 40 (2006) 5355–5366.
3. Kukkonen J.,Pohjola M.,Sokhi R. S., Luhana L.,Kitwiroom N., Fragkou L., Rantamaki M., Berge E. Odegaard V., Slordal L. H., Denby B. and Finadri S., *Atmos. Environ.*, 39 (2005) 2759–2773.
4. Malek E., Davis T., Martin R. S. and Silva P.J., *Atm Res.*, 79 (2006) 108–122.

5. Kerminen V., Pakkanen T. A., Makela T., Hillamo R. E., Sillanpaa M., Ronkko T., Virtanen A., Keskinen J., Pirjila L., Hussein T. and Hameri K., *Atmos. Environ*., 41 (2007) 1759–1767.
6. Hosler C. R., *Mon. Wea. Rev*, 59 (1961), 319–339.
7. Tyson P. D., Preston-Whyte R. A. and Diab R. D.., *S. Afr. Geogr. J.*, 58 (1976) 151–163.
8. Preston-Whyte R. A, Diab R. D. and Tyson P. D., *S. Afr. Geogr. J.*, 59 (1976) 45–59.
9. Milionis A. E. and Davies T. D., *Theor. Appl. Climatol.*, 94 (2008) 225–239.
10. Milionis A. E. and Davies T. D., *Int. J. Climatol.*, 12 (1992) 205–215.
11. Stull R. B., *Kluwer Academic Publishers*, Dordrecht (1988), 666 pp.
12. Fochesatto G. J., Ristori P., Flamant P.H., Ulke A., Nicolini M. and Quel E., Peer reviewed contributions to the *International Laser Radar Conference*, Québec, Canada (2002) 231–234.
13. Curry J. A., *J. Atmos. Sci*., 40 (1983), 2279–2292.
14. Cassano E.N., Cassano J. J. and Nolan M., *J. Geophys. Res*, 116 (2011) D11108. doi:10.1029/2010JD015341.
15. Csanady G. T., *Bound.-Lay. Meteorol*, 6 (1974) 63–79.
16. Mayfield J. A., and G. J. Fochesatto, *J. Appl. Meteorol. Clim.*, 52 (2013) 953–973.
17. Tennekes H., *J. Atmos. Sci*., 30 (1973) 558–567.
18. Taylor J. A. and Yates R. A., 2nd edn, *St. Martin's Press*, New York (1967), 315 pp.
19. Byers H. R., *McGraw Hill*, New York (1974). 461 pp.
20. Kahl J. D., *Int. J. Climatol*., 10 (1990) 537–548.
21. Kahl J. D., Martinez D. A. and Zaitseva N. A., *Int. J. Climatol*., 16 (1996) 1297–1313.
22. Smith F. B. and Hunt R. D., *Atmos. Environ.*, 12 (1977) 461–477.
23. Andre J. C. and Mahrt L., *J. Atmos. Sci*., 39 (1982) 864–878.
24. Mctainsh G. H. and Walker P. H., *Z. Geomorph. N.F*., 26 (1982) 417–435.
25. Adedokun J.A., Emofurieta W.O., Adedeji A.O., *Theoretical and Applied Climatology*, 40 (1989) 161–169.
26. Fochesatto G. J., *Atmos. Meas. Tech*., 8 (2015), 2051–2060.
27. Lothon M., Said F., Lohou F. and Campistrom B., *Mon. Weather Rev.*, 136 (2008) 3477–3500.
28. Blakadar A. K., *Bull. Am. Meteorol. Soc.*, 38 (1957) 283–290.
29. Garratt J. R., *Q. J. R. Meteorol. Soc.* 120 (1994) 1428–1429.

(2017) ; http://www.jmaterenvironsci.com